Effect of Physical Annealing on the Dynamic Mechanical Properties of a High-T_g Amine-Cured Epoxy System

G. WISANRAKKIT and J. K. GILLHAM*

Polymer Materials Program, Department of Chemical Engineering, Princeton University, Princeton, New Jersey 08544

SYNOPSIS

Physical annealing of a fully cured amine/epoxy system has been investigated using the freely oscillating TBA torsion pendulum technique. The material densifies spontaneously during annealing in an attempt to reach equilibrium, thereby changing material behavior. The dynamic mechanical behavior of a film specimen (T_g = 174°C, 0.3 Hz) and of a glass braid composite specimen (T_g = 182°C, 0.9 Hz) was monitored during isothermal annealing at sub-T_g temperatures (ranging to 230°C below T_g); after annealing, the behavior was measured vs. temperature and compared with that of the unannealed state. Isothermally, the storage modulus (G') of the film specimen and the relative rigidity ($1/P^2$) of the composite specimen increased almost linearly with log time, whereas the logarithmic decrement (Δ) decreased with time. The isothermal rates of annealing were determined from the rates of changes in G' and in $1/P^2$ for the film and composite specimens, respectively. In a wide temperature range between T_g and the secondary transition temperature, T_{sec} ($\approx$ −30°C, 2.3 Hz by TBA), the isothermal rates of annealing at the same annealing time appeared to be the same. Thermomechanical spectra of the isothermally annealed material revealed a maximum deviation in thermomechanical behavior from the unannealed material in the vicinity of the annealing temperature. The effects of physical aging were the same for the film and composite specimens. Effects of sequential annealing at two isothermal temperatures on the thermomechanical behavior were also investigated; when the second temperature was higher than the first, the effect of only the high-temperature annealing was evident, whereas the effect of annealing at both temperatures was revealed when the second temperature was lower than the first. Results suggest that physical annealing at different temperatures involves different length scales of chain segment relaxation and that the effects of isothermal aging can be eliminated by heating to below T_g.

INTRODUCTION

Recent studies in our laboratory on high T_g amine-cured epoxy systems have investigated the decrease of the room temperature (RT) modulus and of the RT density that eventually occurs with increasing extent of cure (i.e., T_g).[1-3] For example, Figure 1 shows the anomaly in terms of sequential dynamic mechanical torsional braid analysis (TBA) temperature scans of a partially cured specimen and of the fully cured specimen. Note that the relative rigidity ($\sim$ shear modulus) at room temperature of the undercured specimen (i.e., with lower T_g) is higher than that of the fully cured specimen (see caption to Fig. 1). An explanation has been proposed that attributes an increasing free volume in the glassy state at RT to the nonlinear increase of T_g with conversion.[3] An alternative explanation depends on the efficiency of spontaneous densification in the glass transition region being higher for lower T_g material.[3] It is therefore pertinent to investigate the effect of T_g on annealing (physical aging). The present study deals with the annealing behavior of fully cured specimens as a background for studies on undercured materials.

It is well documented that amorphous polymers can lock in excess free volume during temperature cooling through T_g due to the rapid rise in viscosity,

* To whom correspondence should be addressed.

Journal of Applied Polymer Science, Vol. 42, 2465–2481 (1991)
 CCC 0021-8995/91/092465-17$04.00

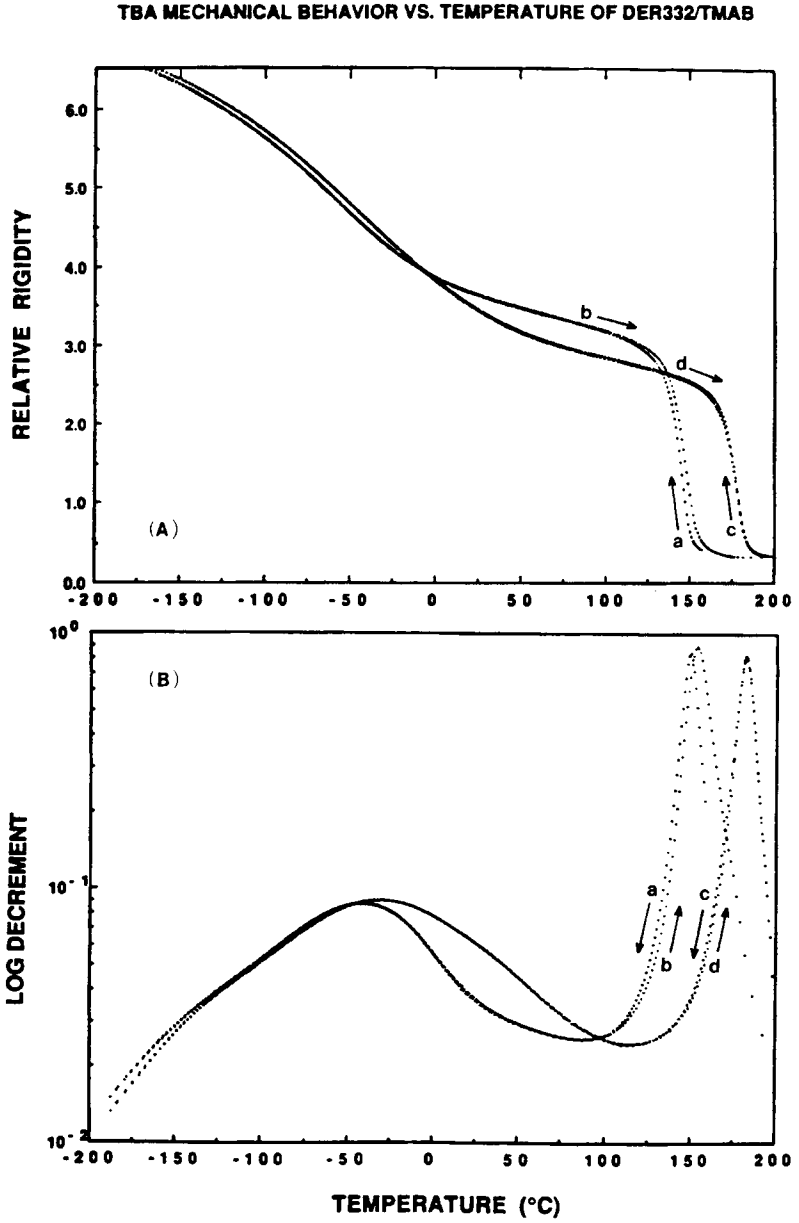

Figure 1 TBA dynamic mechanical properties vs. temperature: (A) relative rigidity, (B) logarithmic decrement. Curves (a) and (b) are for a specimen partially cured at 160°C for 2 h. Curves (c) and (d) are for the fully cured specimen. The sequential TBA temperature scans in helium at 1°C/min are (a) 160 → −180°C, (b) −180 → 250°C, (c) 250 → −180°C, and (d) −180 → 250°C (data above 200°C not shown). Notes: (1) The Tg of the partially cured specimen increases during heating to 250°C due to additional chemical reaction. (2) The RT relative rigidity of the undercured specimen is higher than that of the fully cured specimen. For a specimen that vitrifies (i.e., $T_g \geq T_{cure}$) during isothermal cure, sub-T_g annealing at the cure temperature could also occur and could contribute to the increase in RT rigidity.[3] However, in this example, the undercured specimen did not vitrify during the isothermal cure; therefore, physical annealing did not occur during cure. (3) The relative rigidity of the fully cured specimen becomes higher than that of the undercured specimen in the temperature range below 0°C. This may be attributed to the shift in the secondary transition [< 0°C] to a higher temperature for the fully cured specimen, which causes its relative rigidity to again cross that of the undercured specimen.

which prevents the polymer chain segments from attaining equilibrium conformations.[4,5] The long-term properties of these materials in the glassy state have been amply demonstrated to change when the materials are annealed below T_g.[6-12] This behavior reflects the tendency of the polymer chain segments to slowly approach equilibrium conformations in the glassy state. The approach toward equilibrium has been viewed as a recovery process and has been explained in terms of volume relaxation,[6] enthalpy relaxation,[7-11] and reduction of molecular mobility.[12] The rate of annealing depends on the time and temperature of annealing. Thermoplastics become more rigid and more brittle with annealing.[4,12] Similarly, graphite/epoxy composites show a trend toward decreasing strain-to-break and decreasing toughness.[13,14]

Our recent preliminary annealing studies[15,16] on epoxy systems using the TBA technique have shown that sub-T_g annealing of high T_g epoxies affects thermomechanical properties mostly in the vicinity of the annealing temperature, and, in particular, annealing at temperatures well above room temperature does not significantly change the dynamic mechanical properties of the material at room temperature.[15] The studies have also demonstrated that the TBA technique can be a useful and sensitive way for monitoring the physical annealing process over a wide temperature range through the changes in mechanical properties (namely, relative rigidity and logarithmic decrement) that are presumably closely related to the specific volume of the material. The effect of isothermal annealing on material behavior is made apparent by comparing temperature scans of isothermally annealed specimens with those of unaged material. A glass braid supporting the material (in the TBA specimen), as well as crosslinking in a homogeneous film specimen, makes it possible to erase the prior annealing effects by taking the material to above its glass transition temperature so that many experiments can be performed using the same specimen.

This paper presents results of further annealing studies on a fully reacted amine-cured epoxy system using the TBA torsion pendulum technique. The dynamic mechanical properties of the material both in the form of a thin rectangular film and a glass braid composite specimen are monitored during isothermal annealing at different temperatures. The behavior vs. temperature after annealing is compared with that of the unannealed state. Effects of sequential annealing at two different isothermal temperatures are also examined.

CHEMICAL SYSTEM

The chemical system used in this study was a mixture of a difunctional epoxy and a tetrafunctional aromatic diamine in a stoichiometric ratio (i.e., one epoxy group per one amine hydrogen). The epoxy monomer was a diglycidyl ether of bisphenol A (DER 332 from Dow Chemical Co.) with an epoxide equivalent weight of 174 g/eq (determined by bromine titration by Dow Chemical Co.). The amine curing agent was crystalline (melting range 125–128°C) trimethylene diaminobenzoate, TMAB (Polarcure 740M from Polaroid Corp.), with an amine equivalent weight of 157 g/eq. The chemical structures of both reactants and the basic chemical reactions involved in the cure are shown in Figure 2.

The amine was dissolved in the liquid epoxy at 100°C (15 min). Immediately after thorough mixing, the warm liquid was degassed for 10 min in a vacuum oven held at RT. The clear viscous liquid was poured into small aluminum weighing pans, individually sealed in plastic bags, kept in a desiccator, and stored in a refrigerator.

EXPERIMENTAL

TBA Torsion Pendulum Technique

All experiments were performed using a single glass braid composite (TBA) specimen and a single thin rectangular homogeneous film torsion pendulum (TP) specimen in separate TBA instruments. The specimen is situated inside a temperature-controlled cylindrical chamber through which passes a continuously flowing atmosphere of inert He gas. Figure 3 shows a schematic diagram of the automated TBA torsion pendulum system.[17-19] The essential component of the instrument is the inner pendulum assembly that consists of a vertical specimen clamped between two straight rods: the upper activation rod and the lower freely suspended pendulum rod. The upper activation rod is connected to a computer-controlled gear mechanism that activates the pendulum into small angle, free oscillation by mechanically slowly stretching and subsequently rapidly releasing a spring. The free end of the lower pendulum rod is magnetically coupled to a polarizer disk, which is a part of the inertial mass of the entire inner pendulum and is suspended over another stationary polarizer. The light intensity from a light source passing through the two polarizers varies linearly with

CHEMICAL REACTANTS

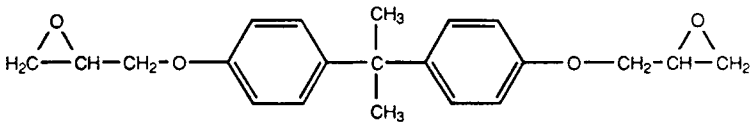

Diglycidyl Ether of Bis-phenol A (DER332, Dow Chemical Co.)

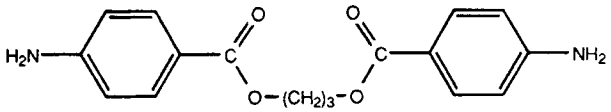

Trimethylene glycol di-p-aminobenzoate (TMAB, Polaroid Corp.)

REACTIONS

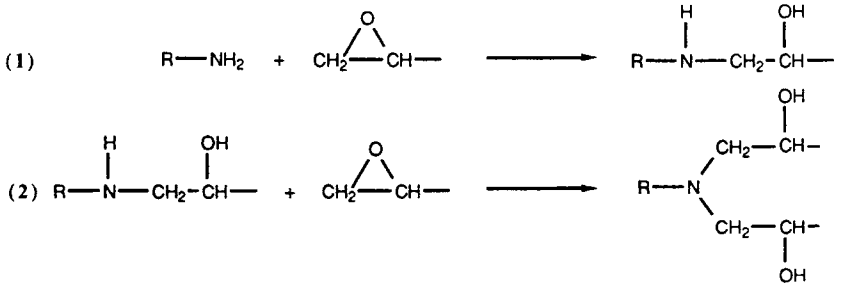

Figure 2 Chemical reactants and reactions.

their relative angular displacement (when in the center of the linear region of the polarizer pair). A linearly responding photo detector converts the light intensity into an analog electrical signal. The analog electrical signal of the freely damped oscillations is digitized and analyzed to give the dynamic mechanical behavior of the specimen with respect to changes in temperature and/or time. The continuously generated analog electrical signal is also used to automate repetitive initiation of the oscillations.

Quantitative values of the elastic modulus and loss modulus can be obtained when specimens of known simple geometry, for example, a rectangular film or a cylindrical filament, are used in the torsion pendulum (TP) mode. The elastic shear modulus, G', is calculated from the frequency (f, Hz) whereas the logarithmic decrement, Δ, which is related to the loss modulus, is calculated from the decay of a damped oscillating wave[17,18]:

$$G' \cong 4\pi KIf^2 = 4\pi KI\left(\frac{1}{P}\right)^2$$

where P (seconds) is the natural period of the damped oscillations, I is the moment of inertia of the moving part of the pendulum, and K is a geometric constant; and

$$\Delta = \ln\left(\frac{\theta_i}{\theta_{i+1}}\right) \cong \pi \frac{G''}{G'} = \pi \tan \delta$$

where θ_i is the amplitude of the ith oscillation of the freely damped wave, G'' is the loss shear modulus, and δ is the phase angle between stress and strain. Calibration (for determining G') must first be performed to determine the moment of inertia of the inner pendulum[21] using a calibrated wire of known moment of inertia.

Impregnated braid specimens are used in the torsional braid analysis (TBA) mode to obtain transitions and relative mechanical assessments of polymers.[17-19] Although the geometric constants are not known in a TBA experiment, the frequency of a damped wave can be used to calculate the relative modulus, since $G' \sim f^2 = 1/P^2$. Two parameters

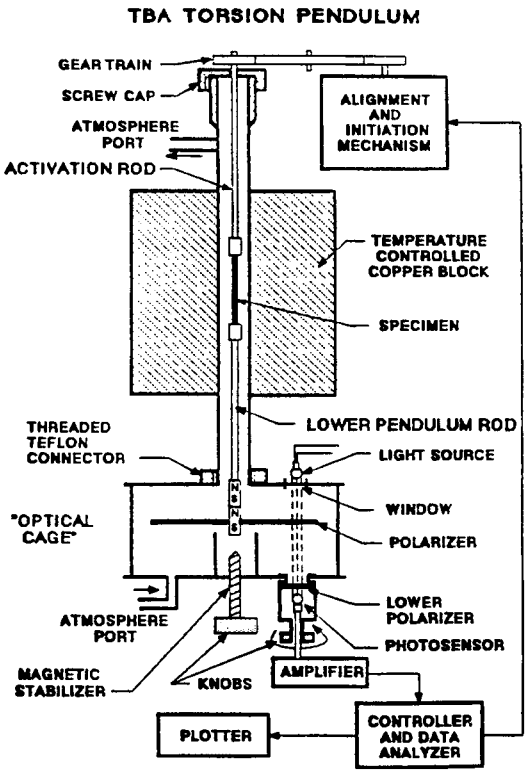

Figure 3 Schematic diagram of the TBA torsion pendulum system. Source: Plastics Analysis Instruments, Inc., Princeton, NJ.

are generally calculated for a TBA experiment, namely, the relative rigidity, $R = 1/P^2$, and the logarithmic decrement, Δ ("log decrement").

Preparation, Cure, and Annealing of Specimens

Composite TBA Specimen

Prior to an experiment, the reactive mixture inside its plastic bag was removed from the refrigerator and left at room temperature for at least 20 min. The viscous reactive liquid was then coated on a heat-cleaned glass braid (ca. 50 mm in length) to prepare the composite specimen for the TBA experiment. Excess material on the braid was removed by squeezing the impregnated glass braid between aluminum foil. The final amount on the braid was approximately 15 mg. The specimen was mounted in the TBA inner pendulum assembly, which was then lowered into the preheated chamber of a TBA instrument.

The specimen was cured in the TBA unit at 200°C for 10 h. After the isothermal cure, the specimen was taken through the following temperature scan: 200 → −180 → 250 → 30°C at 1°C/min, to obtain the thermomechanical spectra after cure. This procedure was adopted because (a) the material could be fully reacted in the absence of vitrification during isothermal cure at 200°C (since T_g of the fully cured system = 182°C), (b) the specimen would be heated to 200°C after subsequent annealing experiments to eliminate the effects of prehistories, and (c) no degradation was observed at 200°C (e.g., the T_g of the material remains constant after more than 100 h at 200°C—results of a separate experiment using a different specimen, not shown here). The cured material was therefore deemed to be chemically stable at 200°C (with respect to chemical conversion and thermal degradation) for the anticipated time scale of the experiment (~ 1 year). Furthermore, the repeated cooling from and heating to 200°C at 1°C/min of the experiment did not affect the thermomechanical spectra and the T_g of the material. All curing and subsequent annealing experiments were performed under a flowing dry helium atmosphere to minimize effects of moisture and oxidation.

Film Specimen

In making the thin film specimen, a thin sheet of partially cured material was prepared as follows: The initial liquid mixture was degassed in a vacuum oven at 100°C and poured between two smooth pads of silicone rubber that were squeezed together with a uniform weight on the top pad; the whole setup was then placed in an air oven at 120°C for 24 h. After the setup had been freely cooled to room temperature, a thin sheet of the partially cured material could be peeled from the silicone rubber pads. The sheet was then cut with scissors into several rectangular strips. A strip with approximately uniform thickness was selected as the film specimen for the present TP annealing study. The specimen was mounted in the usual manner, inserted into the TBA instrument, and fully cured by heating to 200°C at 0.2°C/min and holding isothermally at 200°C for 10 h in helium. Then, it was subjected to the temperature scan 200 → −180 → 200 → 30°C at 1°C/min to obtain the thermomechanical spectra after cure. The average dimensions of the cured specimen (measured at RT after completion of all annealing experiments) were 6.7 × 0.69 × 0.013 cm^3.

Annealing Procedure

A fully reacted specimen (composite or film) was taken to 200°C and then cooled at a rate of 5°C/min to a prespecified annealing temperature (T_a) below T_g. The material was allowed to anneal iso-

thermally at T_a, while its dynamic mechanical behavior was repetitively monitored for exactly 10,000 min. The temperature was maintained at T_a to within ±0.1°C after an initial transient period of approximately 20 min. At the end of 10,000 min, the specimen was cooled from T_a to −180°C and then heated to 200°C, both at 1°C/min, to obtain the dynamic mechanical behavior of the annealed material vs. temperature. Subsequent cooling from 200°C (which is above the specimen's T_g) to −180°C and then heating to 200°C, both at 1°C/min, provided thermomechanical spectra that were compared with those of the annealed, and also the unannealed material obtained immediately after curing. The latter provided an internal means of checking for any irreversible change accompanying the annealing and further temperature cycling. Annealing was performed at different temperatures (ranging from −50 to 180°C). Prior to each new annealing experiment, the specimen was heated to 200°C to erase the previous annealing history and cooled to the new annealing temperature at 5°C/min. Adopting this procedure, one specimen of each type (composite and film) was used for all of the experiments.

Effects of sequential isothermal annealing at two different temperatures were also examined. Each specimen (TBA composite or film) was annealed at the first temperature (T_{a1}) for 10,000 min after cooling at 5°C/min; then the temperature was changed to a new annealing temperature (T_{a2}) at 5°C/min. The specimen was allowed to anneal at T_{a2} for 10,000 min. After the combined annealing sequence, the specimen was subjected to the following temperature cycle: $T_{a2} \rightarrow -180 \rightarrow 200 \rightarrow -180$°C at 1°C/min, so as to obtain the dynamic mechanical behavior of the specimen vs. temperature. In one set of experiments, $T_{a1} > T_{a2}$; in another set, $T_{a1} < T_{a2}$.

RESULTS AND DISCUSSION

The dynamic mechanical behavior of the TBA specimen is reported as the relative rigidity ($1/P^2$) and logarithmic decrement (Δ). The results of the thin film specimen are reported as the storage shear modulus (G') and the logarithmic decrement (Δ).

Thermomechanical Spectra of the Fully Cured Specimen

Figure 4(A) shows the dynamic mechanical behavior vs. temperature of the TBA specimen for both directions of temperature change after curing at 200°C for 10 h before isothermal annealing. The T_g of the material (identified as the maximum of the highest temperature peak in the logarithmic decrement spectrum on temperature scanning down from 200°C) is 182°C (0.9 Hz). The secondary (β) transition is centered around −30°C (2.3 Hz). It is noted that the spectra measured during the temperature scan down do not coincide with those obtained during the temperature scan up. Specifically, the rigidity of the latter is slightly higher and the logarithmic decrement is slightly lower than those of the former in the lower temperature region of the glass transition. These differences could be the consequence of (a) the temperature scan rate at 1°C/min being slow enough to allow the material to anneal to a small extent during cooling and subsequent heating and/or (b) a systematic temperature difference between heating and cooling of about 1°C (see below).

Figure 4(B) shows the similar behavior vs. temperature of the fully cured TP film specimen. The T_g of the specimen is determined (during a temperature scan down from 200°C) to be 174°C (0.3 Hz), which is significantly lower than that of the composite specimen. The difference may arise from degradation during cure in the air oven at 120°C for 24 h or be due to the composite nature of the TBA specimen. The specimen was expected to be chemically stable for all subsequent heating, cooling and annealing experiments that were conducted inside a TBA apparatus under a continuous slowly flowing He atmosphere.

Reversibility of the Physical Annealing Phenomenon

Figure 5(A) shows the thermomechanical spectra of the composite specimen, after having been annealed at 140°C for 10,000 min and heated to 200°C, measured during a temperature scan down at 1°C/min from 200°C (which is above its T_g), compared with the spectra of the same specimen prior to all annealing experiments (also measured from 200 to −180°C at 1°C/min). The spectra of the annealed specimen after heating to 200°C coincide completely with those of the unannealed specimen. Similar behavior is observed for the film specimen, after annealing at 145°C for 10,000 min, cooling to −180°C, and heating to 200°C, as shown in Figure 5(B). These observations indicate that thermal annealing histories below the glass transition temperature can be erased by heating the material to above its T_g and that no irreversible changes (e.g., additional chemical conversion, thermal degradation, and

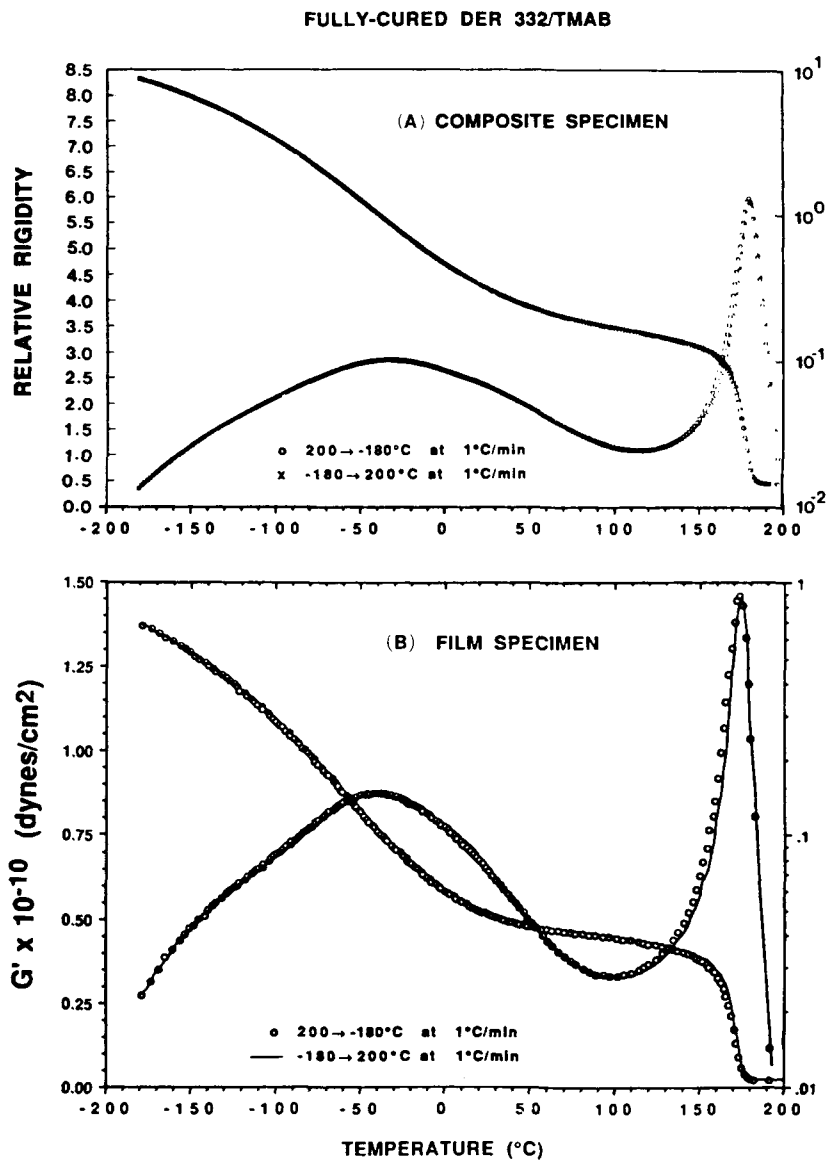

Figure 4 Dynamic mechanical properties vs. temperature of the fully cured material during sequential temperature scans 200 → −180 → 200°C at 1°C/min: (A) composite specimen, (B) film specimen. See text.

physical effects such as crazing or cracking) occur during isothermal annealing and subsequent temperature scans. Therefore, the initial state of the specimen prior to physical annealing can be reproduced by simply heating the material 20°C above its T_g. Consequently, annealing behavior at different temperatures could be examined on single specimens (composite and film).

Isothermal Annealing Behavior

The levels of the initial relative rigidity and shear modulus of unannealed specimens decrease monotonically with increasing temperature. During isothermal annealing, the rigidity and shear modulus increase with annealing time. Figures 6 and 7 show the relative rigidity and G' during isothermal annealing at different annealing temperatures for the composite and the film specimen, respectively. Note that the vertical scale in Figure 6 has been expanded more than 24 times over that for Figure 5(A), and the scale in Figure 7 is 30 times that of Figure 5(B). The results clearly demonstrate the nonequilibrium nature of the material even at temperatures far below T_g (up to 230°C below T_g). In principle, the

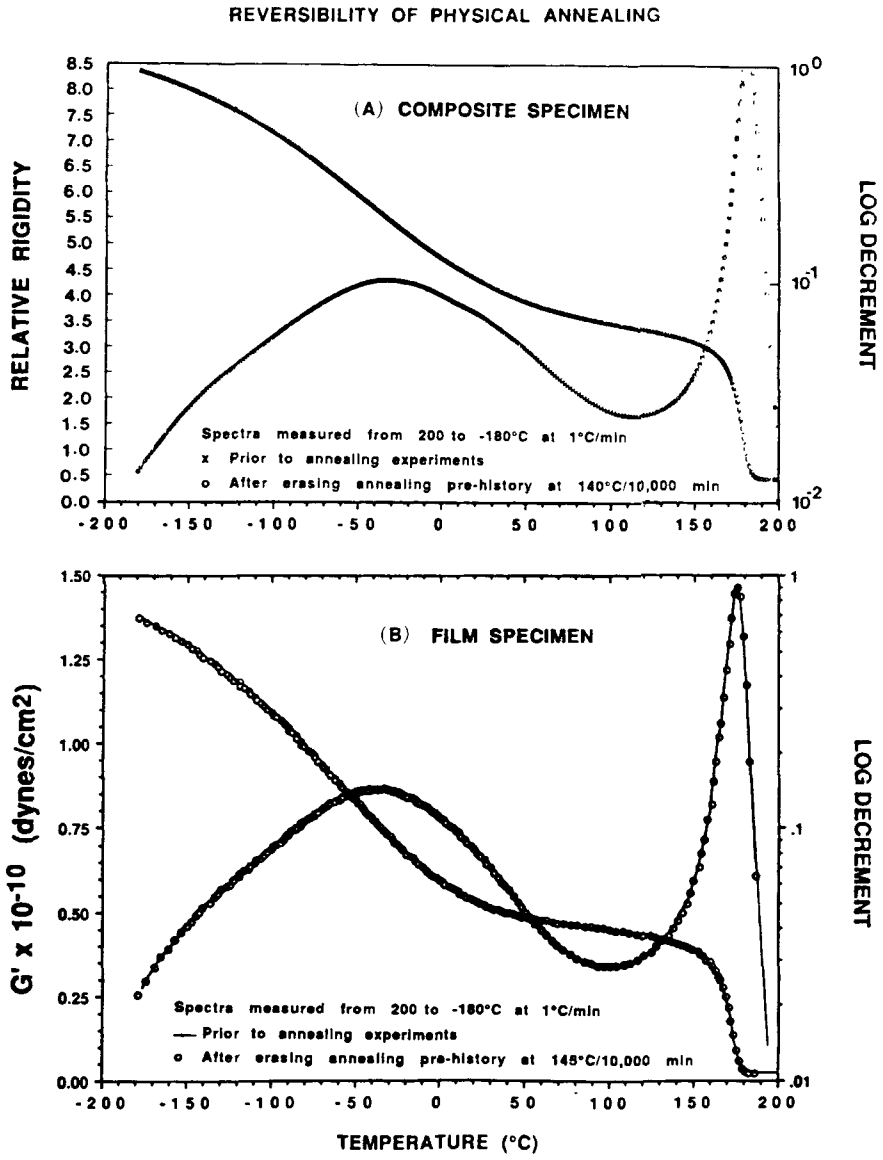

Figure 5 Dynamic mechanical spectra (from 200°C to −180°C at 1°C/min) showing the reversibility of physical annealing effects. The spectra of a specimen prior to the annealing experiment are superimposed over the spectra of the same specimen after annealing at 140°C for 10,000 min and heating to 200°C prior to scanning: (A) composite specimen, (B) film specimen. Note that the spectra for each specimen overlap completely.

material will eventually reach its equilibrium state and the changes would level off after prolonged annealing times. This is actually observed at annealing temperatures close to T_g, for example, at 175°C for the composite specimen (Fig. 6) and at 165°C for the film specimen (Fig. 7). For temperatures near T_g, the equilibrium state can be achieved rapidly since the relaxation times are short and the material is close to equilibrium.[3,8] For all of the annealing temperatures greater than 20°C below T_g in this study, the properties of the material (for both the composite and film specimens) are still changing at the end of the 10,000 min. Figures 8(A) and 8(B) show the behavior of the composite and the film specimens during annealing at 160 and 145°C, respectively, for a longer time period of 45,000 min (~ 1 month). It is apparent that neither specimen has reached its equilibrium state.

It is noticed from Figure 6 that the relative rigidity data at 175°C (i.e., T_g − 7°C) and 180°C (i.e., T_g

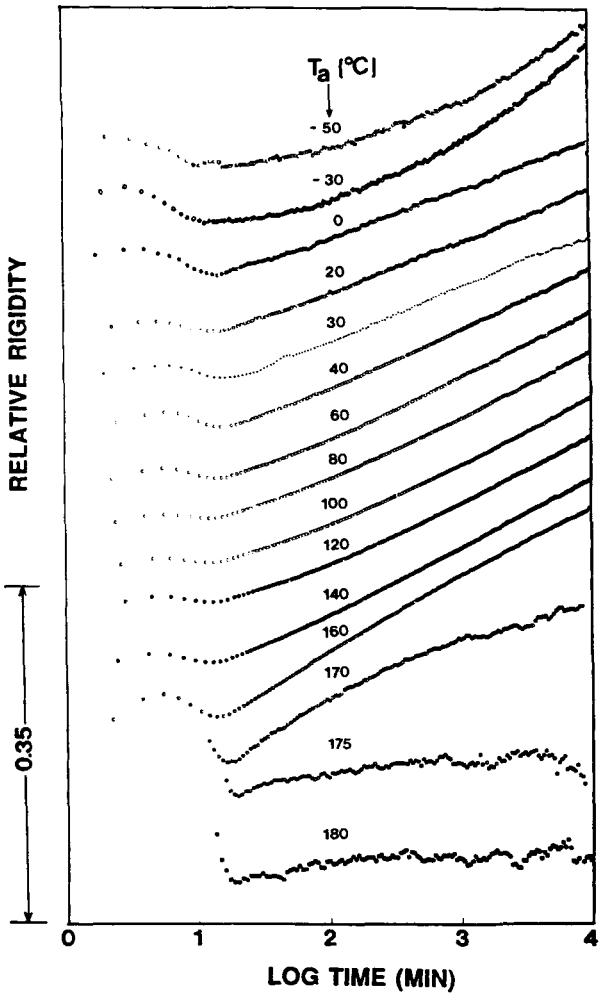

Figure 6 The relative rigidity of the composite specimen vs. log time during isothermal annealing at different annealing temperatures (from −50 to 180°C). The sets of data are displaced vertically from each other by arbitrary amounts. The vertical scale is expanded more than 24× that of Figure 5(A).

− 2°C) display more scatter than those at lower annealing temperatures. The reason for this scatter is that at these temperatures close to T_g the material properties are highly sensitive to small temperature fluctuations (even though the temperature is controlled to within ±0.1°C). Moreover, the dynamic behavior of the specimen becomes viscous with a highly damped response of a few oscillations for a freely damped wave. Therefore, calculations of the material properties from these responses can be less accurate than from the less damped waves at lower temperatures.

Many studies including small strain creep,[12] dynamic mechanical,[3] stress relaxation,[5,9] enthalpy relaxation,[7,8] volume relaxation,[22] and dielectric relaxation[23] experiments have shown that physical aging at long time is linear with respect to logarithmic aging time. These results also showed that physical aging is not highly temperature dependent, at least in the temperature range between T_g and T_{sec}.

Studies by Petrie[7,8] on polystyrene demonstrated that changes in dynamic mechanical properties (i.e., shear storage modulus [G'] and logarithmic decrement) can be correlated with the enthalpy relaxation for samples with the same annealing histories. If enthalpy relaxation is equivalent to volume relaxation, the shear storage modulus and the relative

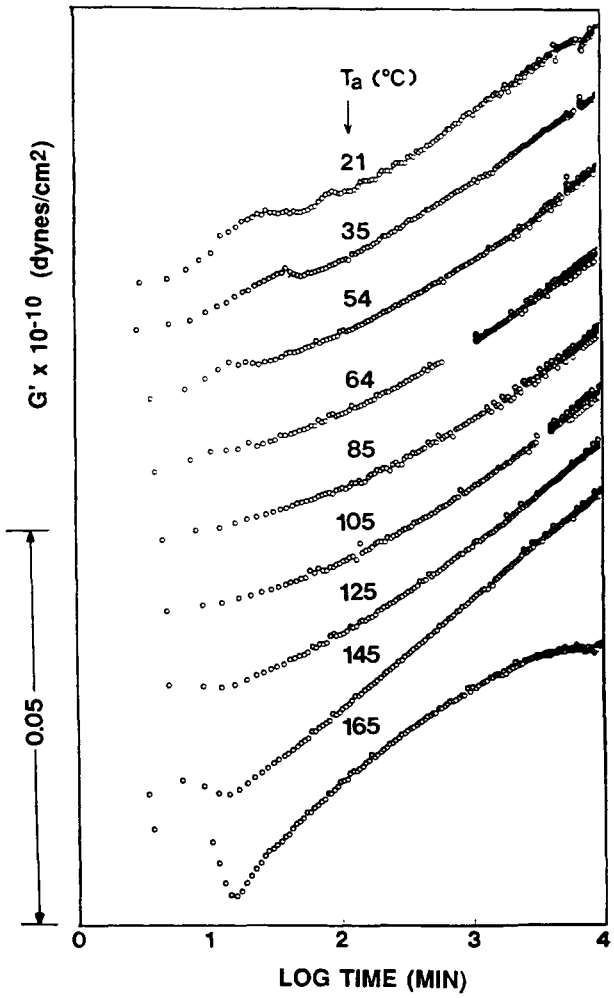

Figure 7 The dynamic elastic shear modulus (G') of the film specimen vs. log time during isothermal annealing at different annealing temperatures (from 21 to 165°C). The sets of data are displaced vertically from each other by arbitrary amounts. The vertical scale is expanded 30× that of Figure 5(B).

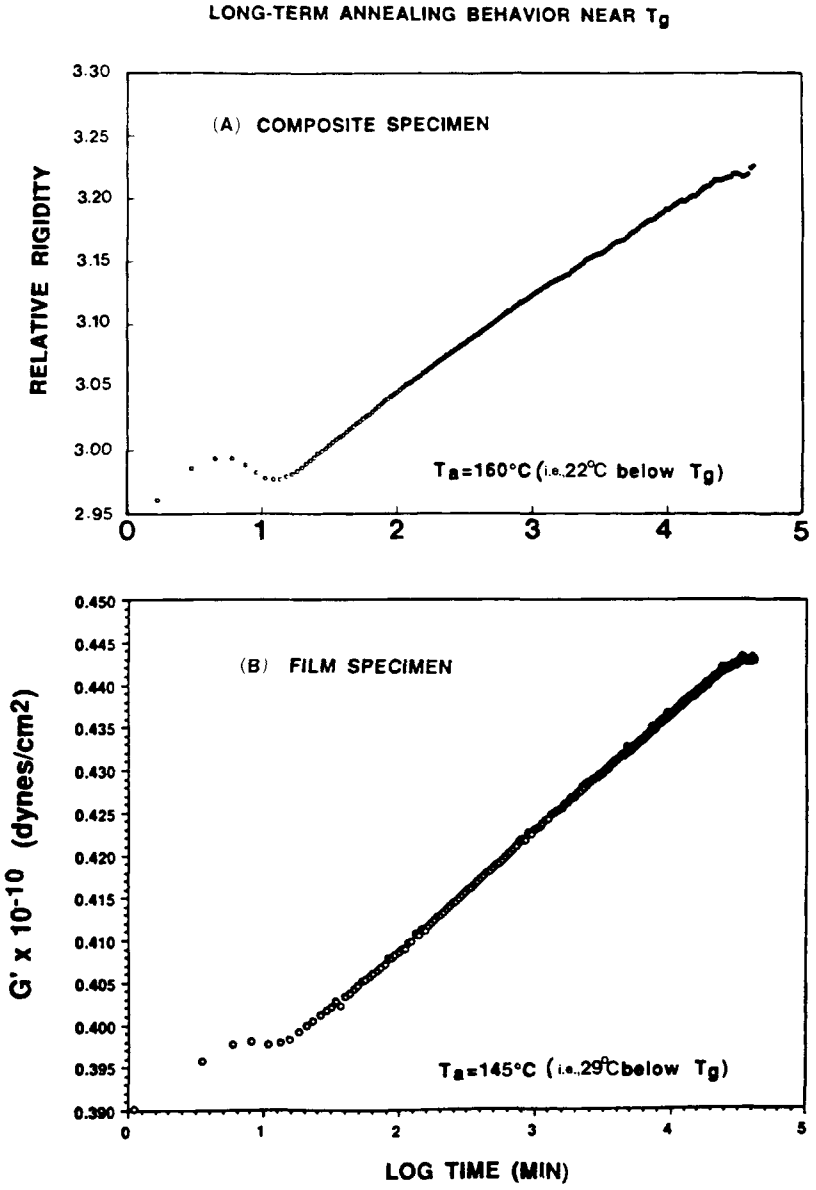

Figure 8 Long-term ($\approx$ 1 month) isothermal annealing behavior near T_g: (A) composite specimen, T_a = 160°C (i.e., 22°C below T_g), (B) film specimen, T_a = 145°C (i.e., 29°C below T_g).

rigidity would be then closely related to the specific volume of a material. The rate of physical annealing (i.e., volume relaxation) could then be inferred from the rates of change of these properties.

It can be clearly seen from Figures 6 and 7 that the long-time rigidity, R, of the composite specimen and the long-time G' of the film specimen, away from equilibrium, increase almost linearly with logarithmic annealing time, t. The data at each annealing temperature, excluding the initial 20 min which are affected by temperature transients, are fitted with a second-order polynomial in log(time) that is used in the evaluation of the rate of annealing. The rate of annealing is calculated as dR/dt for the composite specimen and as dG'/dt for the film specimen. The results of the annealing rates for the composite and the film specimen are shown in Figures 9(A) and 9(B), respectively. It can be observed that the rate of annealing changes inversely with the annealing time. As expected, the initial rate of annealing is higher at temperatures closer to T_g and is lower at temperatures below the secondary transition temperature, T_{sec}. However, in a wide temperature range between T_g and T_{sec}, the rates of annealing appear

to be the same. These observations are in accordance with other investigations in the literature.[3,12]

The similar behavior of the annealing rates versus time in the temperature range between T_g and T_{sec} of the composite and the film specimen suggests that annealing is due primarily to the polymer matrix; the glass braid in the composite specimen contributes little effect to the annealing behavior. In fact, the rate of annealing versus time, in this temperature range where the rate of annealing is independent of temperature, for the film specimen, dG'/dt, is approximately linearly proportional to that of the composite specimen, dR/dt, as shown in Figure 10.

Dynamic Mechanical Behavior vs. Temperature after Annealing

The spectra of the relative rigidity and logarithmic decrement vs. temperature obtained during the temperature scan $T_a \rightarrow -180 \rightarrow 200 \rightarrow -180 \rightarrow$

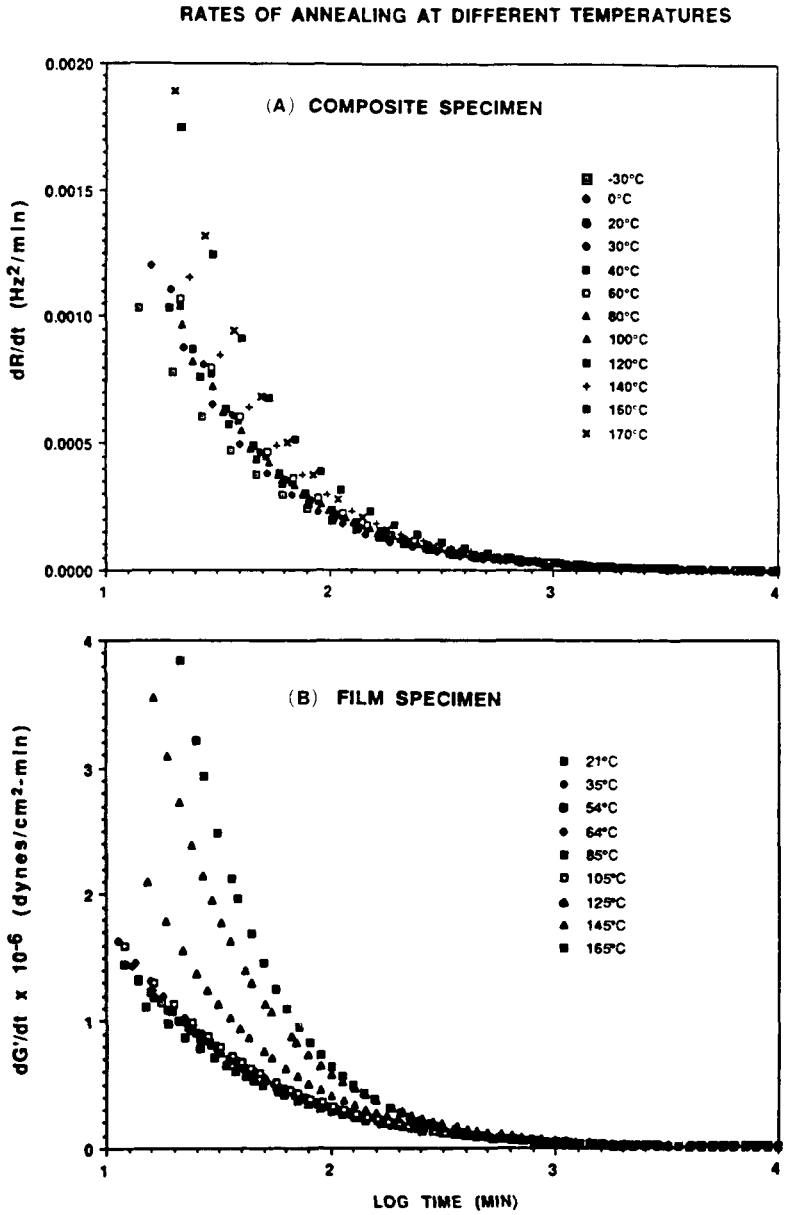

Figure 9 Isothermal rates of annealing vs. log time at different annealing temperatures determined as (A) dR/dt for the composite specimen and (B) dG'/dt for the film specimen. Note that the rates of annealing in a wide temperature range between T_g and T_{sec} appear to be the same.

200°C at 1°C/min of a specimen after annealing at various temperatures are summarized in Figures 11 and 12, respectively. The corresponding spectra of the shear modulus and logarithmic decrement of the film specimen obtained during the temperature scan $T_a \rightarrow -180 \rightarrow 200 \rightarrow -180$°C at 1°C/min are summarized in Figures 13 and 14, respectively. The results of the initial temperature sequence $T_a \rightarrow -180 \rightarrow 200$°C represent the thermomechanical behavior of the annealed specimen; the spectra of the same specimen during cooling from 200 to −180°C are taken as the behavior in the unannealed state, which are shown as solid curves for comparison.

The differences between thermomechanical spectra of annealed and unannealed specimens are found to be most pronounced in the vicinity of the annealing temperatures, in which the mechanical properties of the former (higher rigidity and lower logarithmic decrement) deviate most from the latter. The results at annealing temperatures ≥ 30°C show that the physical annealing does not seem to significantly affect the mechanical spectra of the material below or above the vicinities of the annealing temperatures. The localization of the effect suggests that (1) the submolecular motions which are responsible for the aging effect at T_a and which are gradually immobilized over long times at T_a are not involved in determining G' in the time scale of ~1 s for $T < T_a - 30$°C and (2) the submolecular motions that had been immobilized by the annealing process at T_a are freed by volume expansion on raising the temperature so that G' in the time scale of −1 s at $T > T_a + 30$°C is not affected by the annealing at T_a. This argument suggests that the length scale of the motions which are effective in the annealing process at different annealing temeratures, T_a, vary with T_a and that only intermediate

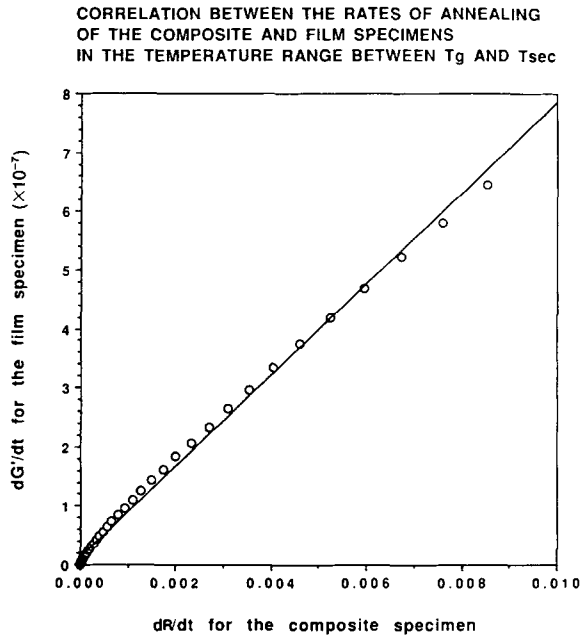

Figure 10 Rates of annealing in the temperature range between T_g and T_{sec} of the film specimen (dG'/dt) plotted vs. that of the composite specimen (dR/dt) to examine the contribution of the glass braid to the annealing behavior. See text.

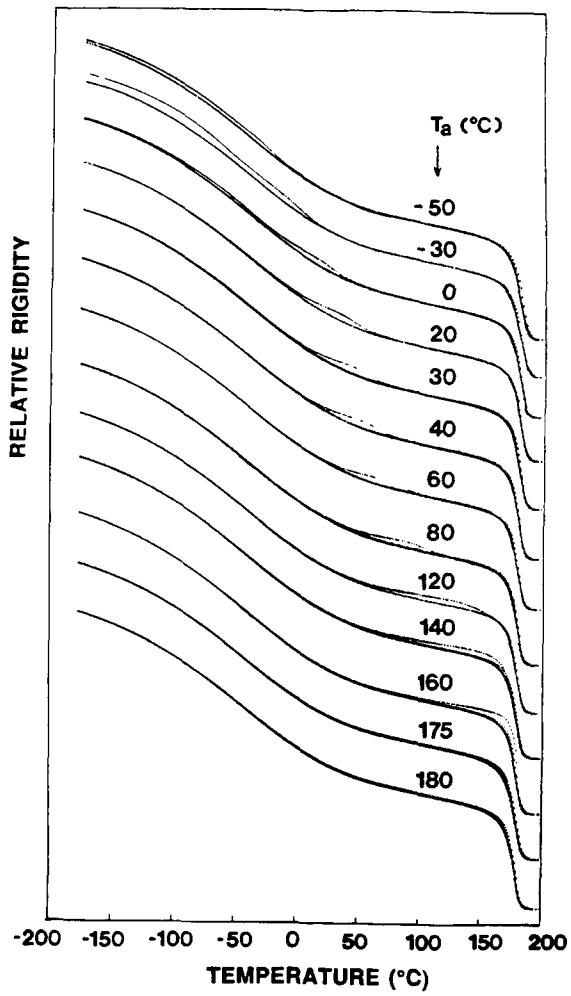

Figure 11 Relative rigidity vs. temperature of the annealed composite specimen at different annealing temperatures (Ta) compared with that of the same specimen in the unannealed state. Annealing was for 10,000 min at each temperature. The dotted curves show the spectra of the specimen, after annealing at T_a, from $T_a \rightarrow -180 \rightarrow 200$°C, whereas the corresponding solid curves give the spectra of the unannealed state of the same specimen from 200 to −180°C (the subsequent scan from −180 to 200°C is shown also as dotted curves). Note the regions of maximum perturbation are in the vicinities of the isothermal annealing temperatures (for $T_a \geq 0$°C).

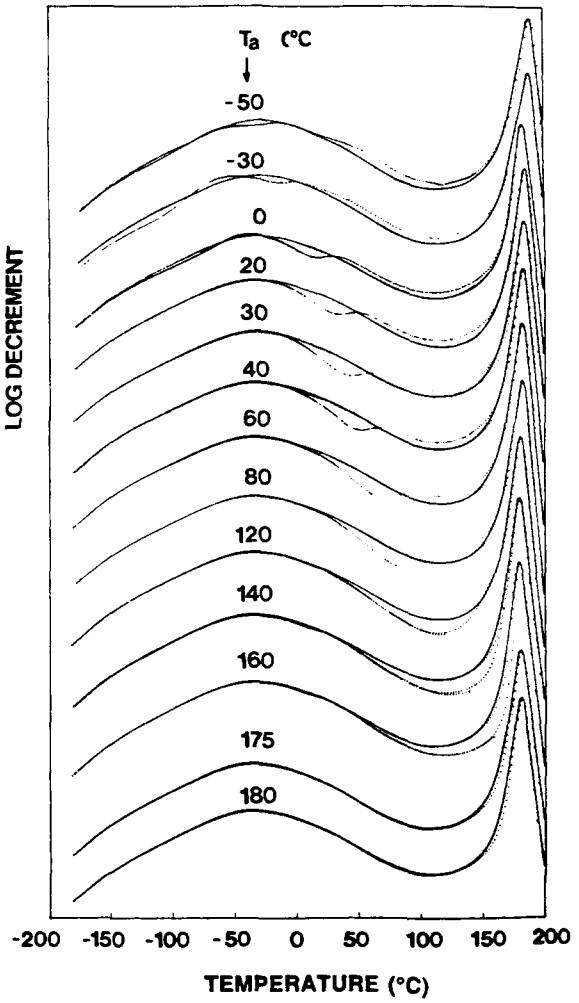

Figure 12 *Logarithmic decrement vs. temperature of* the annealed composite specimen at different annealing temperatures compared with that of the same specimen in the unannealed state. (See caption of Fig. 11.)

regions of the relaxation spectrum are involved at a given temperature.

However, the annealing effect is quite different at annealing temperatures at and below 0°C; the thermomechanical spectra of an annealed specimen appear to differ substantially from the unannealed spectra throughout the entire temperature range of the glassy state below the annealing temperatures. A related issue on sub-T_g annealing studies concerns the effect of physical annealing on the secondary transition, T_{sec} (TBA) ≈ -30°C (2.3 Hz). There have been reports that physical annealing does not significantly affect the secondary transition,[24-26] although other reports suggest otherwise.[27,28] The present results show that annealing at high temperatures does not significantly affect the secondary transition. However, the annealing results at low temperatures close to the secondary transition peak (e.g., −50 to 0°C in Figs. 11 and 12) show that the secondary relaxation can be substantially influenced by physical aging in the vicinity of T_{sec}. For example, the annealing at −30°C (where the logarithmic decrement peak of the secondary transition is at its maximum) also results in higher rigidity (Fig. 11) and lower logarithmic decrement (Fig. 12) in the vicinity of T_{sec}.

Effect of Physical Annealing on T_g

Table I shows values of the T_g of the composite specimen, obtained during temperature scans after

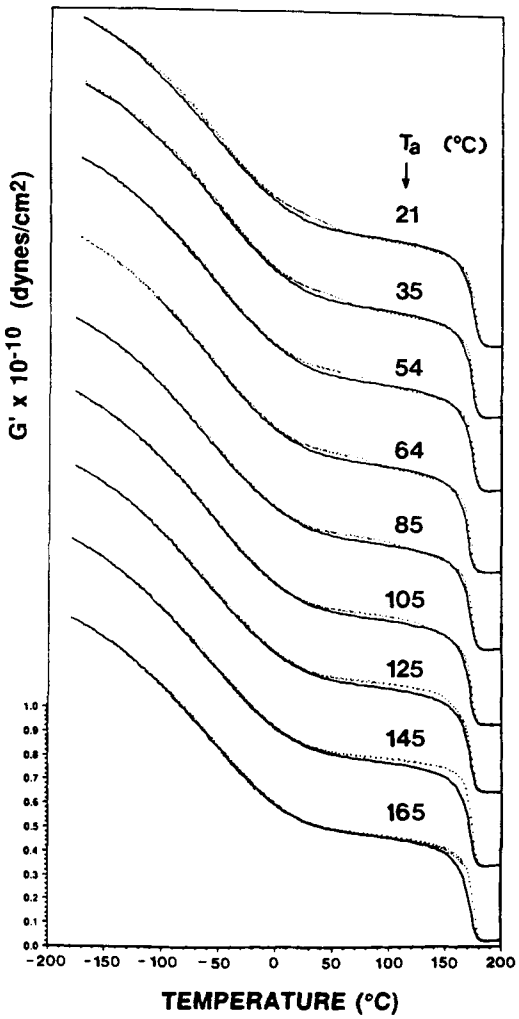

Figure 13 Sheer modulus vs. temperature of the annealed film specimen compared with that of the same specimen in the unannealed state. The dotted curves show the spectra of the specimen after annealing at T_a, from $T_a \rightarrow -180 \rightarrow 200$°C, whereas the corresponding solid curves give the spectra of the unannealed state of the same specimen during subsequent scanning from 200 to −180°C.

Table I T_g of the Composite Specimen after Annealing Experiments

T_a (°C)	−180 → 200°C	200 → −180°C	−180 → 200°C	200 → 30°C
−50	182.9	182.1	182.9	182.0
−30	183.0	182.1	183.1	182.1
0	182.5	181.7	182.5	181.7
20	182.6	181.7		
30	182.6	181.6	182.4	181.7
40	182.6	181.9	182.7	181.7
60	182.6	181.8	182.6	181.7
80	182.5	181.6	182.5	181.6
100	182.5	181.6	182.6	181.7
120	182.3	181.5		
140	182.4	181.7	182.5	181.7
160	183.1	182.0	182.9	181.9
175	183.0	182.1	183.0	182.1
180	182.9	181.8	182.8	181.8
120/60	183.0	182.0	182.9	182.1
60/120	182.8	181.9	182.7	182.0
140/40	182.8	182.0	182.9	182.0
40/140	182.9	182.0	183.0	182.0

each annealing experiment at T_a. Each value is determined by curve fitting of the T_g peak in the logarithmic decrement spectrum to a second-order polynomial that is used to calculate the maximum ($\equiv T_g$). The values in the second column represent the T_g of the annealed specimen, which has been cooled to −180°C at 1°C/min, measured during the subsequent temperature scan from −180 to 200°C at 1°C/min. The values in the third, fourth, and fifth columns represent the T_g of the same specimen in the unannealed state measured during the consecutive temperature scans 200 → −180, −180 → 200, and 200 → 30°C at 1°C/min, respectively. The value of T_g measured during a temperature scan down is approximately 0.9°C lower than that measured during a temperature scan up (comparing the T_g values in column 3 with those in column 4). The differences in T_g values between cooling and heating scans presumably arise from thermal lag between the specimen and the measuring temperature (on cooling the specimen is at a higher temperature than the thermocouple; on heating, the specimen is at a lower temperature than the thermocouple). Comparison between scans must therefore be made in the same direction of temperature change. Furthermore, since physical annealing at sub-T_g temperatures does not affect the value of the assigned T_g (comparing the T_g values in column 2 with those in column 4), this implies that the annealing histories have virtually been erased when the temperature reaches the assigned value of T_g. Thus, by this particular way of defining T_g (i.e., from the peak of the logarithmic decrement), physical annealing does not change the temperature assigned to T_g.

Table II Sequence of Temperatures in the Step-annealing Experiments

Experiment	T_{a1}/T_{a2} (composite specimen)	T_{a1}/T_{a2} (film specimen)
1	120/60°C	125/64°C
2	60/120°C	64/125°C
3	140/40°C	145/35°C
4	40/140°C	35/145°C

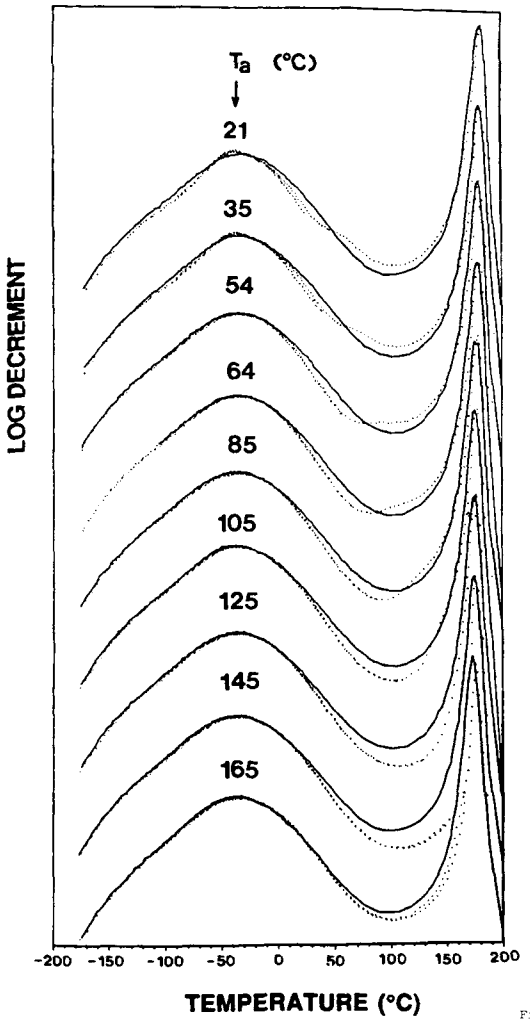

Figure 14 Logarithmic decrement vs. temperature of the annealed film specimen at different annealing temperatures compared with that of the same specimen in the unannealed state. (See caption of Fig. 13.)

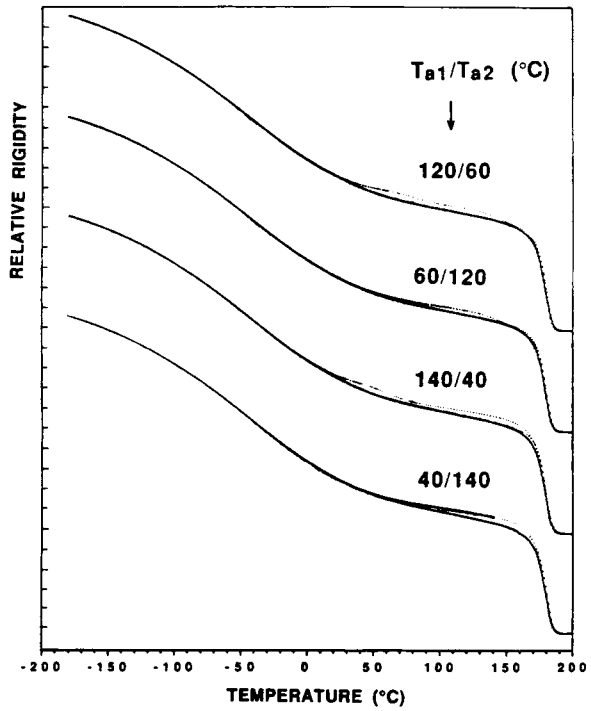

Figure 15 Effects of the sequential annealing at two sub-T_g annealing temperatures on the relative rigidity of the composite specimen during the temperature sequence: $T_{a2} \rightarrow -180 \rightarrow 200$°C (dotted lines) and $200 \rightarrow -180$°C (solid lines). The two numbers (T_{a1}/T_{a2}) next to each spectrum are the two annealing temperatures in the order of the annealing experiment (10,000 min at each temperature). The initial cooling rate to T_{a1} was 5°C/min. The temperature scan rate from T_{a1} to T_{a2} was 5°C/min.

Effect of Sequential Isothermal Annealing

The results of sub-T_g isothermal annealing at temperatures above 20°C show that there is a range of maximum perturbation in the vicinity of the annealing temperature in the thermomechanical spectra of the annealed material as compared to the unannealed state. Therefore, it is of interest to examine the effects of sequential isothermal annealing at two different temperatures on the perturbation behavior.

Four sets of experiments were performed on each of the two types of specimen. The annealing temperatures for each set of the experiments are given in Table II. Specimens were annealed for 10,000 min at each specified temperature.

In experiments 1 and 3, the first annealing temperatures were higher than the second temperatures, whereas in experiments 2 and 4, the reverse temperature sequences were carried out. The initial cooling rates from 200°C to T_{a1} were 5°C/min. The heating and cooling rates from T_{a1} to T_{a2} were 5°C/min.

After each experiment, the relative rigidity (or G') and the logarithmic decrement of the specimen were obtained during a temperature scan $T_{a2} \rightarrow -180 \rightarrow 200 \rightarrow -180$°C at 1°C/min. The results are presented in Figures 15 and 16 for the relative rigidity and logarithmic decrement spectra of the composite specimen and in Figures 17 and 18 for the G' and logarithmic decrement spectra of the film specimen, respectively.

For experiments 1 and 3, in which $T_{a1} > T_{a2}$, the resulting thermomechanical spectra appear to be a combination of separate annealing at T_{a1} and T_{a2}. The regions of maximum perturbation from the unannealed state appear in the vicinities of both T_{a1} and T_{a2}. In experiments 2 and 4, the specimen was heated to a higher second annealing temperature: the mechanical spectra after the sequential annealing only reflect the characteristics of the second annealing temperature with the region of maximum perturbation occurring only in the vicinity of T_{a2}.

These results again suggest that physical annealing at different temperatures involves different scales of relaxations. An annealed state attained at a higher temperature is unaffected by subsequent annealing at a lower temperature that may only involve relaxations of chain segments and free volume

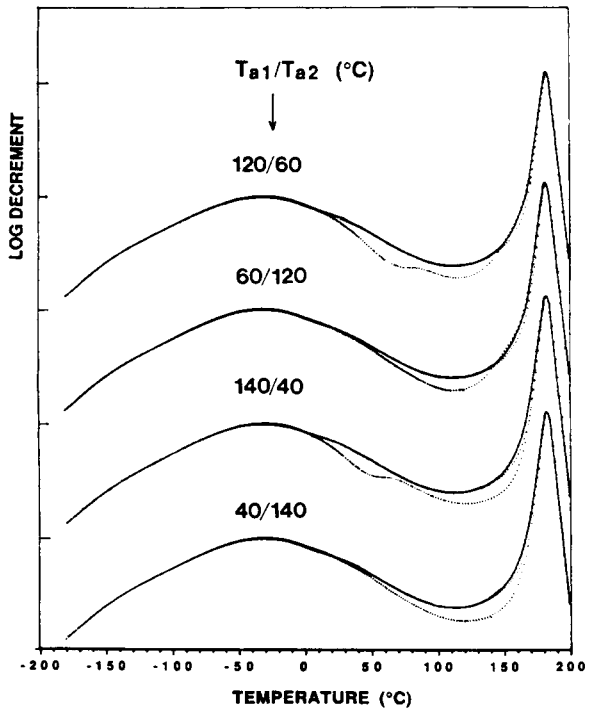

Figure 16 Logarithmic decrement vs. temperature of the composite specimen showing the effect of the sequential annealing at two sub-T_g annealing temperatures. (See caption of Fig. 15.)

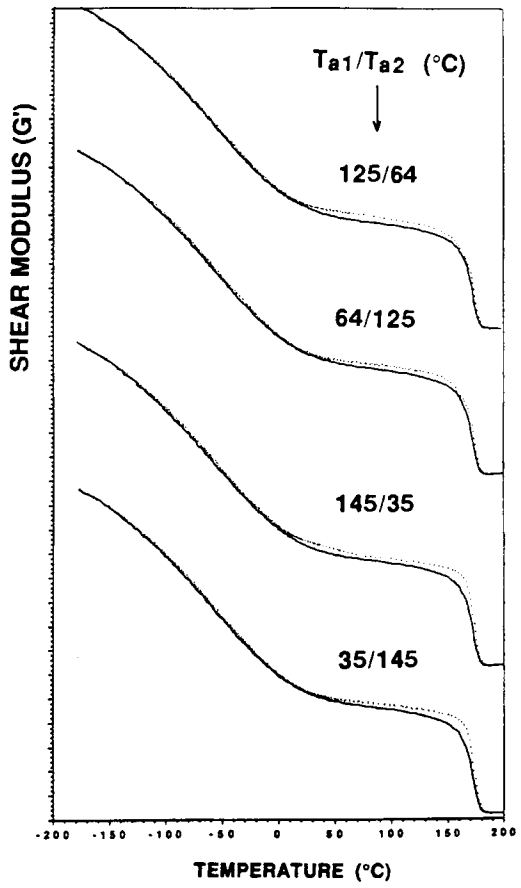

Figure 17 Sheer modulus vs. temperature of the film specimen showing the effect of the sequential annealing at two sub-T_g annealing temperatures. (See caption of Fig. 15.)

of smaller dimensions. On the other hand, the annealing effects at low temperature can be erased (by increasing free volume and shortening relaxation times) when the temperature is raised to a higher temperature. Subsequent annealing at the higher temperature involves the relaxation of longer chain segments (and therefore larger scale volumes) that include those of smaller scale. Consequently, the net result of the combined annealing when $T_{a2} > T_{a1}$ is as though the material has only been annealed at the second (upper) temperature.

CONCLUSIONS

Technique

The torsional braid analysis technique, both in the supported specimen (TBA) and in the suspended film (TP) modes, is a convenient and sensitive method for monitoring the physical annealing process for the following reasons:

1. The changes in the dynamic mechanical properties are presumably related to the changes in the specific volume of the material. The changes of the former can be several orders of magnitude greater than those of the latter and, thus, can be detected more easily.
2. The sensitivity of the freely vibrating, freely suspended specimen is revealed by comparing the isothermal annealing data (e.g., Figs. 6 and 7) with scale expansion > 30 times, with those of the conventional presentation [e.g., Fig. 5(A) and 5(B)]. The technique can effectively monitor small changes in the material's properties, e.g., changes less than 3% in relative rigidity during isothermal annealing.
3. Prior annealing prehistories can be erased by taking the specimen to above its T_g (i.e., physical annealing is a thermoreversible process). Therefore, comparisons of the effects

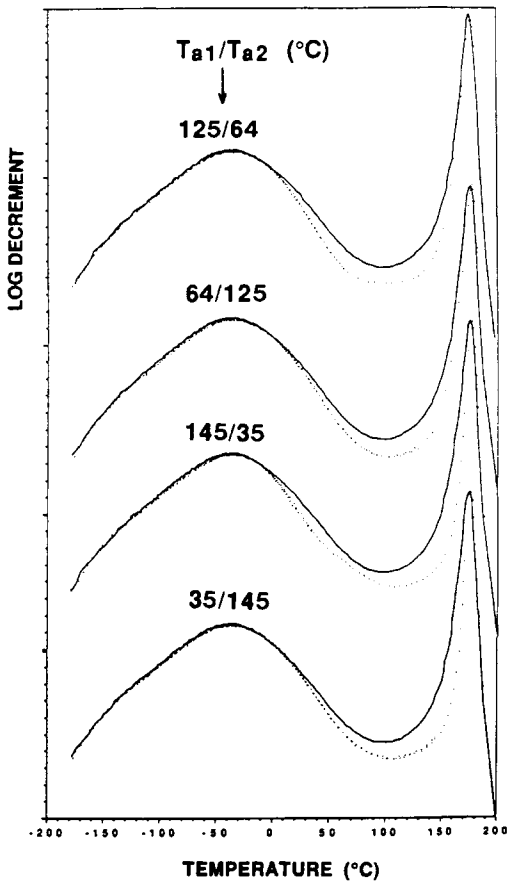

Figure 18 Logarithmic decrement vs. temperature of the film specimen showing the effect of the sequential annealing at two sub-T_g annealing temperatures. (See caption of Fig. 15.)

of time and temperature of annealing can be made using a single specimen.

Results

1. During prolonged isothermal annealing ($T_{sec} < T_a < T_g$), the relative rigidity and shear modulus increase almost linearly with log time. The rate of annealing decreases with time.
2. The rate of annealing vs. temperature of annealing is determined from the change in the relative rigidity and G' vs. time. In a wide temperature range between T_g and T_{sec}, the material appears to anneal at the same rate versus time.
3. Temperature scans of material annealed at one temperature ($T_{sec} < T_a < T_g$) show that its thermomechanical spectra deviate pronouncedly from those of the unannealed state only in the vicinity of the annealing temperature.
4. This suggests that different length scales of relaxation are associated with different annealing temperatures. At lower annealing temperatures closer to T_{sec}, the physical annealing shows substantial effect throughout the glassy state below the annealing temperatures.
5. A specimen that has been annealed at one temperature and subsequently annealed at a lower temperature displays the annealing effects of both temperatures, i.e., the thermomechanical spectra show regions of maximum perturbation in the vicinities of both annealing temperatures. However, if the sequence of the annealing temperatures is reversed, (i.e., first annealing at a low temperature, then at a high temperature), the net result only reflects the annealing effects of the higher temperature. These results again suggest that different scales of relaxation are associated with different annealing temperatures.

This research was supported in part by the Chemistry Branch of the Office of Naval Research.

REFERENCES

1. J. B. Enns and J. K. Gillham, *J. Appl. Polym. Sci.*, **28,** 2831 (1983).
2. M. T. Aronhime and J. K. Gillham, *J. Appl. Polym. Sci.*, **31,** 3589 (1986).
3. K. P. Pang and J. K. Gillham, *J. Appl. Polym. Sci.*, **37,** 1969 (1989).
4. S. E. B. Petrie, *Polymer Materials: Relationships between Structures and Mechanical Behavior*, E. Baer and S. B. Radcliffe, Eds., American Society for Metals, Metal Park, OH, 1975.
5. S. Matsuoka, H. E. Bair, S. S. Bearder, H. E. Kern, and J. T. Ryan, *Polym. Eng. Sci.*, **18,** 1073 (1978).
6. A. J. Kovacs, *J. Polym. Sci.*, **30,** 131 (1958).
7. S. E. B. Petrie, *Bull. Am. Phys. Soc.*, **17,** 373 (1972).
8. S. E. B. Petrie, *J. Polym. Sci.*, **10**(A-2), 1255 (1972).
9. Z. H. Ophir, J. A. Emerson, and G. L. Wilkes, *J. Appl. Phys.*, **49**(10), 5032 (1978).
10. A. R. Berens and I. M. Hodge, *Macromolecules,* **15,** 756 (1982).
11. M. G. Wyzgoski, *J. Appl. Polym. Sci.*, **25,** 1455 (1980).
12. L. C. E. Struik, *Physical Aging in Amorphous Polymers and Other Materials*, Elsevier, New York, 1978.
13. E. S. W. Kong, *J. Appl. Phys.*, **52**(10), 5921 (1981).
14. E. S. W. Kong, *Epoxy Resin Chemistry II*, R. S. Bauer, Ed., Am. Chem. Soc. Symp. Ser. 221 and 171, American Chemical Society, Washington, DC, 1983.
15. K. P. Pang and J. K. Gillham, *J. Appl. Polym. Sci.*, **38,** 2115–2130 (1989).
16. G. Wisanrakkit and J. K. Gillham, *Soc. Plast. Eng., 47th Tech. Conf. Proc.*, 1150 (1989): Also *Amer. Chem. Soc., Prepr. Div. Polym. Sci. Eng.*, **62,** 766 (1990).
17. J. K. Gillham, in *Development in Polymer Characterisation-3,* J. V. Dawkins, Ed., Applied Science Publishers, London, UK, 1982, Chap. 5.
18. J. B. Enns and J. K. Gillham, Am. Chem. Soc. Adv. Chem. Ser. 203, *Polymer Characterization*, C. D. Craver, Ed., American Chemical Society, Washington, DC, 1983, pp. 27–63.
19. J. B. Enns and J. K. Gillham, Am. Chem. Soc. Prep. Div. Polym. Mat. Sci. Eng., **59,** 851 (1989).
20. S. L. Rosen, *Fundamental Principles of Polymer Materials*, Wiley-Interscience, New York, 1982, Chap. 18.
21. L. T. Manzione, U. C. Paek, C. F. Tu, and J. K. Gillham, *J. Appl. Poly. Sci.*, **27,** 1301 (1982).
22. K. C. Rusch, *J. Macromol. Sci. Phys.*, **B2**(2), 179–204 (1968).
23. M. Uchidoi, K. Adachi, and Y. Ishida, *Polymer. J.*, **10,** 161 (1978).
24. L. C. E. Struik, *Polymer,* **28,** 57 (1987).
25. J. L. Gomez Ribelles, and R. Diaz Calleja, *Polym. Eng. Sci.*, **24,** 1202 (1984).
26. A. F. Yee and M. T. J. Takemari, *J. Polym. Sci. (Phys.),* **20,** 205 (1982).
27. G. P. Johari, *J. Chem. Phys.*, **77**(9), 4619 (1982).
28. E. J. Roche, *Polym. Eng. Sci.*, **23,** 390 (1983).

Received December 8, 1989
Accepted August 2, 1990